Webology (ISSN: 1735-188X)
Volume 17, Number 3, 2020

The Couple Of Spherical Particles In A Liquid Show To A Standing Bulk Acoustic Wave (B.A.W).

Shashi Shekhar Vidyarthi

Department of Physics, J.L.N College Dehri-on-Sone V.K.S.University, Ara. India.

ABSTRACT

The interparticle force between two particles exposed to a standing bulk acoustic wave and suspended in a liquid is clarified. By deducting the time-averaged primary radiation force caused by the effect of scattering from the time-averaged total radiation force caused by the combined scattering and re-scattering effects, a three-dimensional model based on the perturbation technique and tensor integral method is used to predict the interparticle force. The findings demonstrate that the interparticle force is attractive, symmetric, and scales with the product of wavenumber (k) and interdistance regardless of the sizes of the particles at the nodal plane. We discover that the interparticle force is dependent on the horizontal (parallel to the nodal plane) and vertical interdistances by examining the interparticle force between two particles that are not on the nodal plane. Our findings demonstrate that the conflict between time-averaged second-order pressure and velocity terms causes the interparticle force to switch from attractive to repulsive at a crucial interdistance. We exposed that the interparticle force is unaffected by the separation between two particles that are parallel to the nodal plane. We present a method for the experimental measurement of the interparticle force and consider the total radiation force as the sum of the interparticle force, axial primary force, and drag force. The interparticle force predicted by the model agrees well (within 5%) with the experimental results. Our research clarifies interparticle forces, enabling more precise calculation of forces acting on particles in an acoustic field.

Keywords: piezoelectric transducer, interparticle force, bulk acoustic wave.

INTRODUCTION.

The creation of an effective method for trapping and manipulating droplets, particles, and cells that is delicate, contactless, and biocompatible is still a challenge despite the considerable developments in microfluidics technology.[1,2]. It is known as acousto microfluidics to use acoustic waves in microfluidics to manipulate tiny particles exclusively based on their mechanical properties. This technique has been shown to have the aforementioned quality[3,4]. A piezoelectric transducer (PZT) is used to create an acoustic standing wave inside a microchannel in a bulk acoustic wave (BAW) based microfluidic device. This standing wave causes objects to experience an acoustic radiation force as a result of the scattering effects[5] The main and interparticle (secondary) radiation forces can be generically classified as two components of acoustic forces depending on scattering. The incident's scattering is primarily responsible for the primary radiation force. As opposed to this, the interparticle (secondary)

force that a particle feels is caused by the re-scattering of waves from the particle in question and its nearby particles. Since the primary force is zero at the pressure node, the interparticle force takes over and can affect how the particles move and are oriented[6,7] Depending on the density and compressibility of the particles, the suspension of the medium, the angle formed by the line connecting the centres of the two particles, and the direction in which the standing wave is propagating, the force may be entirely positive or repulsive. The variation in acoustic energy density along the microchannel's length may result in an axial primary radiation force for a number of reasons, including spatial variation in the energy density across the PZT, variation in the coupling's (the epoxy layer between the transducer and the device) thickness, and nonuniformity in the channel's width. The experimental set-up and simulation model are schematically shown, together with the dynamical behaviour that results from the various forces acting on two particles of equal and different sizes. The principal acoustic radiation force, which is a time-averaged force, is experienced by a particle suspended in a fluid and exposed to an auditory standing wave. Gor'kov provided the following expression for the primary acoustic radiation force for an ideal fluid and a one-dimensional standing wave: Numerous factors, such as the spatial variation in channel width during construction, the spatial variation in energy density across the resonator, the thickness of the coupling (epoxy) layer between the resonator and the silicon chip, etc., can be blamed for the spatial variation of energy density.

The particle size r, position x, and gradient of Eac are shown to affect the axial primary radiation force, Fpx, which tends to propel the particles towards the area of maximal acoustic energy density and will be higher for larger particles. The transverse primary radiation force (along the path of the standing wave), Fpy, is typically stronger than the axial primary force Fpx. The transverse primary acoustic radiation force disappears at the pressure nodal plane, but the axial primary force increases and can have an impact on particle motion. In addition to the aforementioned primary radiation forces, a force known as the secondary or interparticle radiation force, which results from the standing wave's re-scattering from particle surfaces, also occurs between two or more particles. In the literature, numerous formulations for the interparticle (secondary) radiation force have been put forth. The interparticle radiation force between two particles in an ideal fluid aligned parallel to the nodal plane in the direction of the line connecting the centres of the particles is expressed as under uniform acoustic fields.

$$Fpy = -4\pi r\ 3\ Eack\phi\ \sin(2ky),$$

Where Eac is the acoustic energy density, r is the particle radius, ϕ is the contrast factor, k is the wavenumber, and y is the distance of the center of the particle from the pressure node.

$$\phi = 1 - \kappa p/\ \kappa f + 3(\rho p - \rho f)\ /2\rho p + \rho f.$$

In addition to the above, an axial primary force Fpx is generated due to the spatial variation of acoustic energy density, which is expressed as follows:

$$Fs = -\ EacV\ 2\ 0\ \pi\delta 2\ (\ 3(\rho p/\rho f - 1)\ 2\ \sin 2\ (kx)\ 2\delta\ 2 + k(1 - \kappa p/\kappa f)\ 2\ \cos\ 2\ (kx)),$$

Where V0 is the volume of the particle and δ is the center-tocenter interparticle distance. Here, the negative sign indicates that the interparticle force is attractive. It is quite difficult to incorporate into the formulation the hydrodynamic forces brought on by the confinement effect (such as wall effects).41 Additionally, our approach for estimating the contact force between the particles neglects short-range interaction forces, such as lubricating force and van der Waals force, which may be significant when the interparticle distance reaches the order of nanometers. By comparing our model predictions with our experimental data and predictions from an existing model, we have validated our model in the current study. the various forces acting on a pair of particles are shown schematically. The positions of the particles in a pair are arbitrarily chosen to be (x/2, y1) and (x/2, y2), where x is the horizontal distance (i.e., along the nodal plane) between the particles and y1 and y2 are the vertical distances (i.e., normal to the nodal plane) of particles 1 and 2, respectively, from the nodal plane. For x = 0 and y = 1, 2, 0 and both the main and interparticle forces will be present. The interparticle force will be repellent when the particles are farther away from the nodal plane (y1,2 > c) and attracting when they are closer (y1,2 c). When x = 0, the particles are positioned normal to the nodal plane, along the path of the external acoustic wave, where the interparticle force is insignificant, Fs 0, and the particles are only subject to the primary acoustic force. When y1,2 = 0, the particles are in the nodal plane, where the principal acoustic force disappears and they are subject to an attractive interparticle force that is dependent on the distance between the particles. In order to anticipate the interparticle forces between the two particles mentioned above, we provide a numerical model. In tests, the particles may additionally be exposed to the axial primary force due to variations in acoustic energy density, in addition to the transverse primary force (in the direction of the standing wave) and interparticle radiation force. The current study utilised a silicon-based microchannel with dimensions of 370 m in width, 300 m in depth, and 20 mm in length. Pictures of the experimental setup and acousto fluidics chip. The microchannel was through-etched using deep reactive ion etching (DRIE), and the pattern was created using photolithography. Anodic bonding was used to adhere glass slides to the etched substrate on both sides. For inserting the particle suspension within the microchannel, polyethylene tubes were attached at both ends. For particles to migrate and stay at the pressure nodal plane, 5.49 W of power was required.

Experiments were done using polystyrene particles with sizes of 25 m, 15 m, and 10 m to calculate acoustic radiation forces. In order to isolate the beads in the fluid inside the channel for the purpose of examining the forces that the particles interact with acoustically, the bead solution was diluted with deionized (DI) water at a ratio of 1:30 by volume. To explore the interparticle forces between particles of different sizes, the diluted solutions of 25 m and 15 m, 25 m and 10 m were mixed in a 1:1 volume ratio to create the mixed bead solution. High-speed recording is used to capture the movement of particles brought on by acoustic radiation forces. By contrasting the Stokes drag force and the principal acoustic radiation force, the acoustic energy density in the microchannel was determined. Particle positions over time were tracked as they travelled along the transverse plane. We determined the acoustic energy density by equating the Stokes drag force to the main radiation force.

$$Eac = 9\eta\ 4t\phi(kr)\ 2\ \ln[\ \tan[ky(t)]\ \tan[ky(0)]\ ].$$

Where y (0) is the location of the particle in the transverse plane at time t = 0 s, and y(t) is the position of the particle in the transverse plane at time t. is the dynamic viscosity of the suspending medium. Eac is calculated from the aforementioned Eq. (13), using experimentally obtained 10 m particle trajectory fitting data. The energy density is found to be 50 9 J/m3 on average at 5.49 W power, which is utilized to determine the pressure amplitude. The interparticle force, axial primary force, and drag force all balance out at the pressure nodal plane on a pair of equal-sized and unequal-sized particles, respectively (see Fig. 3). The balance of forces on particles 1 and 2 for a pair of particles is determined by the formula b.

$F_{px,1} + F_s - F_{D,1} = 0.$

$F_{px,2} - F_s - F_{D,2} = 0.$

It can be assumed that the particles are initially static and are present in an infinite quiescent fluid since once the particles are put within the microchannel, the flow is stopped. The linear Stokes equation, which has the form FD = 6rU, can be used to approximate the drag force. U is the particle velocity discovered from tracking the positions of the individual particles over time in tests. Due to the particles' low mass, inertial effects are disregarded. Since the particles are in close vicinity, the gradient in the energy density over the distance between the two particles can be neglected. For a pair of equal-sized particles. It is possible to assume that the axial primary radiation force, which relies on the particle size and Eac, is equal, or that Fpx,1 = Fpx,2. The axial primary force and interparticle force between two equal-sized particles can therefore be calculated using the following relations from Eq. (13).\

$F_{px,1} = F_{px,2} = 1\ 2\ (F_{D,1} + F_{D,2}),\ \ F_s = 1\ 2\ (F_{D,1} - F_{D,2})$

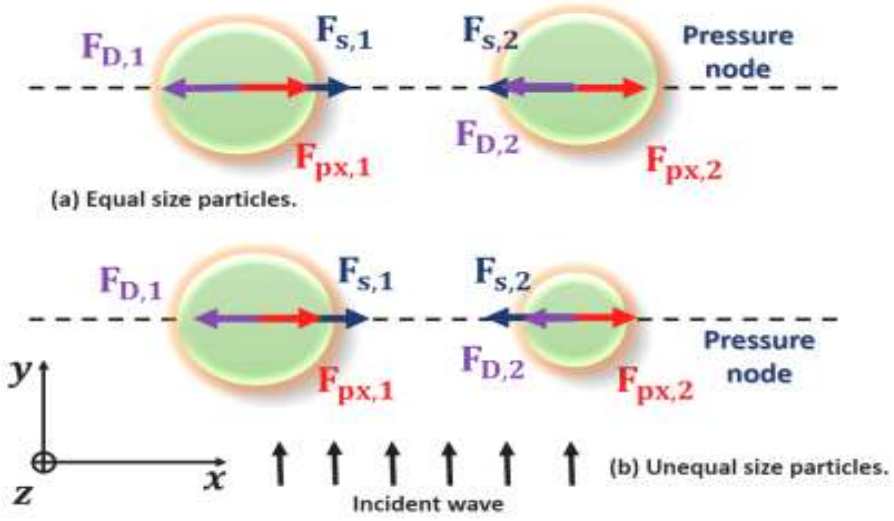

Diagram illustrating the forces that are balanced between two particles of different sizes that are positioned at the nodal plane in the tests.

RESULTS AND DISCUSSION:

The interparticle force between two particles of equal and unequal sizes positioned at the nodal plane, i.e. at (x/2, 0) and (x/2, 0), is initially investigated using the numerical model described in Section III [see Fig. 1(d-iv)]. The particle diameter in the case of two identical particles was determined to be 15 m, 20 m, 25 m, and 30 m. Combinations of particles with sizes of (3 m and 30 m), (10 m and 30 m), and (20 m and 30 m) were taken into consideration in the case of two unequal-sized particles. Sec presents the additional operating conditions utilised in the simulations. a pair was varied such that the product of the wavenumber (k) and the interdistance (δx) was in the range kδx = 0.24 − 0.85. The analytical expression for the interparticle force experienced by a pair of particles located at the nodal plane can be obtained from Eq. (5a) as follows, shows the change of the dimensionless interparticle force (F s) that the numerical model with a dimensionless interdistance (kx) predicted for a pair of equal-sized and unequal-sized particles. The findings demonstrate that, regardless of the particle sizes, the non dimensional interparticle force, which varies with the dimensionless interdistance as F* s = 0.02(kx) 4, is always attractive when the particles are in the nodal plane and agrees with the analytical expression. The findings also demonstrate that, as shown in Fig. interparticle forces experienced by the individual particles in the scenario of a pair of unequal-sized particles are symmetrical, equal in magnitude, and directed in the opposite direction. The forces act on a pair of unequally sized particles with diameters of 10 m and 30 m; the amount of the force acting on the 10 m particle is equal to that on the 30 m particle, but the forces act in different directions. Similar to this, we can see that the force acting on a pair of unequal-sized particles with diameters of 20 m and 30 m is equal to and opposite to the force operating on a particle with a diameter of 20 m. The interparticle forces are attractive because they are both negative (in the x-direction) for particle 1 and positive (along the +x-direction) for particle 2, which are both positioned at (+x/2, 0).

CONCLUSIONS.

The comprehension of the interparticle acoustic radiation forces between two spherical particles exposed to a standing bulk acoustic wave and suspended in a liquid media is presented. To forecast the interparticle forces for a pair of particles positioned arbitrarily near the standing wave, a three-dimensional (3D) numerical model based on the tensor integral approach is created. The time-averaged main acoustic radiation force caused by the scattering effect is subtracted from the time-averaged total acoustic radiation force caused by the combined scattering and re-scattering effects to get the interparticle force. The simulation results demonstrated that the dimensionless interparticle force (F * s) for a pair of equal- and unequal-sized particles positioned at the nodal plane is attractive and symmetric and scales with the product of wavenumber (k) and interdistance between the pair of particles (x), as F* s (kx) 4 in accordance with established theory. We discover that the interparticle force is independent of their placements and only depends on the horizontal (parallel to the pressure node) by investigating the interparticle force between a pair of particles placed outside the nodal plane in various configurations. and inter-vertical distances. According to our findings, the competition between the time-averaged second-order pressure and velocity terms causes the interparticle forces between two particles outside the nodal plane to change from being repulsive to attractive at a critical interdistance of ky 0.13 for kx = 0.26. For a smaller kx, the

distance between the particles at which the maximal repulsive force manifests is greater. In the case of two particles parallel to the nodal plane. Since the existing model only takes into account monopole- and dipole-based velocity potentials and ignores the re-scattering effects that are taken into account in the present model, our numerical model's predictions are more closely matched to the experimental data than those of the existing model, which offers a much better prediction of the interparticle force. Our research illuminates the interparticle forces, making it possible to estimate the forces on particles more precisely and to better understand their dynamical behaviour in an acoustic environment.

REFRENCE

[1] X. Chen and C. L. Ren, "A microfluidic chip integrated with droplet generation, pairing, trapping, merging, mixing and releasing," RSC Adv. 7, 16738 (2017).

[2] H. Sun, Y. Ren, L. Hou, Y. Tao, W. Liu, T. Jiang, and H. Jiang, "Continuous particle trapping, switching, and sorting utilizing a combination of dielectrophoresis and alternating current electrothermal flow," Anal. Chem. 91, 5729 (2019).

[3].A. Lenshof, C. Magnusson, and T. Laurell, "Acoustofluidics 8: Applications of acoustophoresis in continuous flow microsystems," Lab Chip 12, 1210 (2012).

[4].M. Wiklund, "Acoustofluidics 12: Biocompatibility and cell viability in microfluidic acoustic resonators," Lab Chip 12, 2018 (2012).

[5].T. Laurell, F. Petersson, and A. Nilsson, "Chip integrated strategies for acoustic separation and manipulation of cells and particles," Chem. Soc. Rev. 36, 492 (2007).

[6].A. A. Doinikov, "Acoustic radiation forces: Classical theory and recent advances," in Recent Research Developments in Acoustics (Transworld Research Network, India, 2003), Vol. 37661, p. 39.

[7].A. A. Doinikov, "Mutual interaction between a bubble and a drop in a sound field," J. Acoust. Soc. Am. 99, 3373 (1996).

[8].A. A. Doinikov and S. T. Zavtrak, "Interaction force between a bubble and a solid particle in a sound field," Ultrasonics 34, 807 (1996).

[9]. S. M. Woodside, B. D. Bowen, and J. M. Piret, "Measurement of ultrasonic forces for particle-liquid separations," AIChE J. 43, 1727 (1997).

[10]. E. Hemachandran, S. Karthick, T. Laurell, and A. K. Sen, "Relocation of coflowing immiscible liquids under acoustic field in a microchannel," Epl 125, 54002 (2019).

[11]. E. Hemachandran, T. Laurell, and A. K. Sen, "Continuous droplet coalescence in a microchannel coflow using bulk acoustic waves," Phys. Rev. Appl. 044008 (2019).

[12] S. Karthick and A. K. Sen, "Improved understanding of acoustophoresis and development of an acoustofluidic device for blood plasma separation," Phys. Rev. Appl. 10, 034037 (2018).

[13]. S. Karthick and A. K. Sen, “Improved understanding of the acoustophoretic focusing of dense suspensions in a microchannel,” Phys. Rev. E 96, 052606 (2017).

[14]. A. Nath and A. K. Sen, “Acoustic behavior of a dense suspension in an inhomogeneous flow in a microchannel,” Phys. Rev. Appl. 12, 054009 (2019).

[15.N. A. Pelekasis and J. A. Tsamopoulos, “Bjerknes forces between two bubbles. Part 1. Response to a step change in pressure,” J. Fluid Mech. 254, 467 (1993).

[16]. A. A. Doinikov, “Acoustic radiation interparticle forces in a compressible fluid,” J. Fluid Mech. 444, 1 (2001).

[17]. X. Zheng and R. E. Apfel, “Acoustic interaction forces between two fluid spheres in an acoustic field,” J. Acoust. Soc. Am. 97, 2218 (1995).

[18].G. T. Silva and H. Bruus, “Acoustic interaction forces between small particles in an ideal fluid,” Phys. Rev. E 90, 063007 (2014).

[19]. S. Sepehrirahnama, F. S. Chau, and K.-M. Lim, “Effects of viscosity and acoustic streaming on the interparticle radiation force between rigid spheres in a standing wave,” Phys. Rev. E 93, 023307 (2016).

[20].P. Glynne-Jones, P. P. Mishra, R. J. Boltryk, and M. Hill, “Efficient finite element modeling of radiation forces on elastic particles of arbitrary size and geometry,” J. Acoust. Soc. Am. 133, 1885 (2013).

[21]. B. Hammarström, T. Laurell, and J. Nilsson, “Seed particle-enabled acoustic trapping of bacteria and nanoparticles in continuous flow systems,” Lab Chip 12, 4296 (2012).

[22]. R. Habibi, C. Devendran, and A. Neild, “Trapping and patterning of large particles and cells in a 1D ultrasonic standing wave,” Lab Chip 17, 3279 (2017).

[23].A. Garbin, I. Leibacher, P. Hahn, H. Le Ferrand, A. Studart, and J. Dual, “Acoustophoresis of disk-shaped microparticles: A numerical and experimental study of acoustic radiation forces and torques,” J. Acoust. Soc. Am. 138, 2759 (2015).

[24].T. Baasch, I. Leibacher, and J. Dual, “Multibody dynamics in acoustophoresis,” J. Acoust. Soc. Am. 141, 1664 (2017).

[25]. T. Baasch and J. Dual, “Acoustofluidic particle dynamics: Beyond the Rayleigh limit,” J. Acoust. Soc. Am. 143, 509 (2018).

[26] S. Sepehrirahnama, K.-M. Lim, and F. S. Chau, “Numerical study of interparticle radiation force acting on rigid spheres in a standing wave,” J. Acoust. Soc. Am. 137, 2614 (2015).

[27].J. H. Lopes, M. Azarpeyvand, and G. T. Silva, “Acoustic interaction forces and torques acting on suspended spheres in an ideal fluid,” IEEE Trans. Ultrason. Ferroelectr. Freq. Control 63, 186 (2016).

[28] K. Yoshida, T. Fujikawa, and Y. Watanabe, "Experimental investigation on reversal of secondary Bjerknes force between two bubbles in ultrasonic standing wave," J. Acoust. Soc. Am. 130, 135 (2011).

[29]. A. Garcia-Sabaté, A. Castro, M. Hoyos, and R. González-Cinca, "Experimental study on inter-particle acoustic forces," J. Acoust. Soc. Am. 135, 1056 (2014).

[30]. K. A. Johnson, H. R. Vormohr, A. A. Doinikov, A. Bouakaz, C. W. Shields, G. P. López, and P. A. Dayton, "Experimental verification of theoretical equations for acoustic radiation force on compressible spherical particles in traveling waves," Phys. Rev. E 93, 053109 (2016).

[31]. A. R. Mohapatra, S. Sepehrirahnama, and K.-M. Lim, "Experimental measurement of interparticle acoustic radiation force in the Rayleigh limit," Phys. Rev. E 97, 053105 (2018).

[32]. D. Saeidi, M. Saghafian, S. Haghjooy Javanmard, B. Hammarström, and M. Wiklund, "Acoustic dipole and monopole effects in solid particle interaction dynamics during acoustophoresis," J. Acoust. Soc. Am. 145, 3311 (2019).

[33]. L. A. Crum, "Acoustic force on a liquid droplet in an acoustic stationary wave," J. Acoust. Soc. Am. 50, 157 (1971).

[34]. G. Simon, M. A. B. Andrade, M. P. Y. Desmulliez, M. O. Riehle, and A. L. Bernassau, "Numerical determination of the secondary acoustic radiation force on a small sphere in a plane standing wave field," Micromachines 10, 431 (2019).

[35]. R. Barnkob, P. Augustsson, T. Laurell, and H. Bruus, "Acoustic radiationand streaming-induced microparticle velocities determined by microparticle image velocimetry in an ultrasound symmetry plane," Phys. Rev. E 86, 056307 (2012)